American Journal of Applied Sciences 1 (3): 168-175, 2004
ISSN 1546-9239

An Investigation of the Nature Properties of Plasma

[1]Peter Evans, [1]Frederick Osman and [2]Heinrich Hora
[1]School of Quantitative Methods and Mathematical Sciences,
University of Western Sydney, Locked Bag 1797, Penrith South DC 1797, Australia
[2]Department of Theoretical Physics, University of New South Wales, Sydney, 2052, Australia

Abstract: This study presents the characteristics of the plasma and the effect of the laser beam to best suit the plasma model behavior. Special attention is paid to the "Genuine" Two Fluid Model and the ponder-motive and transient forces. These models are translated into a numerical study of the parameters, such as the electric field density and temperature distributions once electromagnetic energy is supplied to the plasma. The parameters are presented graphically against time and distance into a small plasma fuel pellet. It is noted how field density and ions form undulations through the plasma. Types of plasma fuels are discussed with regards to their key parameters, such as density, volume and temperature. These characteristics were initially used in computations that were performed using the laser driven inertial fusion energy option based on volume ignition with the natural adiabatic self-similarity compression and expansion hydrodynamics[1].

Key words: Plasma, Laser Beam, Electric Density, Ion Density

INTRODUCTION

This is a very complex field of study, involving many fields of understanding, electromagnetic field theory, atomic structure and quantum mechanics (noticeably little used or mentioned in the literature.) It deals with the mathematics of gradient fields, the resulting forces, moving charges and the theories of thermo-kinetic movement and especially employs non-linear mathematics. There is an overview at the beginning, of the forces involved and the models of plasma structure. It is too vast an area of knowledge to plough into at this study, without showing such an overview. Coupled with the plasma structure are the values of temperature, energies and densities, etc. Involved. Numerical work is offered in this study dealing with the non-neutrality of plasmas. Specially, the internal 'churning' that goes on inside a plasma, before and during any external fields, such as lasers supplied electromagnetic fields is offered to them.

Debye length and plasma neutrality: One of the first questions to be asked about the nature of the plasma is how far apart are the particles? By particles, what is meant, the ions or ions included with surrounding electrons? In the case of deuterium, one electron for every ion, one proton and accompanying neutron. Indeed this idea of electron and ions leads to an addition to the plasma definition. Looking at it as a dielectric medium whose properties are determined by free charges, with no dipoles involved[2]. This describes fully ionized plasma, a condition that cannot always be considered to be the case.

Table 1: Plasma Properties

Plasma Situation	Electron Density (N)	Temperature » K
Intergalactic Space	10^{-5} per cm^3.	10^5 to 10^6
Interstellar Medium	10^{-3} and 10 per cm^3.	100 weak ionised 10^4 strongly ion.
Solar corona	10^4 and 3×10^8 per cm^3.	10^6
Inter-planetary Space	1 and 10^4 per cm^3. Latter value occurring most when powerful corpuscular emissions occur from the sun.	
Ionosphere	10^3 and 3×10^6 per cm3.	300 to 3,000
Thermo-nuclear Reaction	~10^{15} per cm^3 Estimated by some for controlled fusion.	10^8 to 10^9 Current apparatus it is 10^6 to 10^7.
Various gas discharge apparatus	10^{12} per cm^3.	

Examining some plasma's it can be found that the electron density varies (Table 1)[3].

If there is a density of the electrons, then in neutral plasma that should be approximately the density of the positive ions, there could also be neutral particles, which introduce the idea of the degree of ionization. For example, in Earth's lower D layers of the ionosphere, the neutral particle density is around 10^{15}. The ratio of electron density to neutral particle density is 10^{-11} to 10^{-12}. In the Sun's corona is almost zero. If the plasma is not fully ionized, then $n_e \neq n_i$ electron number will not equal in numbers. This being the case a

potential difference will exist. The average $\bar{V}$ of which, taken at any proper the plasma, can be repressed [ted by Poisson's equation[4,5]:

$$\nabla^2\bar{v} = -\left(n_i - n_e\right)e/\varepsilon_0 \quad (1)$$

On the other hand if the plasma is fully ionized there could be 3N equations for N particles, making up the equipartion function:

$$\begin{aligned} v &= pr_0^{\,2}\left\lfloor 1-\left(r^2/3r_0^{\,2}\right)\right\rfloor/2\varepsilon_0 \quad 0<r<r_0 \\ &= pr_0^{\,2}/3\varepsilon_0 r \qquad\qquad\qquad r>r_0 \end{aligned} \quad (2)$$

The interesting point is that the space-charge fields can actually maintain a condition close to neutrality - Sommerville [6] offers the numerical example of $10^{20}/\ m^3$ of equal electron to ion particles and goes on to show using the above equations that a small electronic movement ends up requiring a field of 10^9V/m, too large to maintain, so conditions close to neutrality are maintained. He establishes departure being no more than a few parts in a million over volumes such as $10^{-9}m^3$.

By examining the proposition of what happens when a test charge is placed in it, the particle, being an iron, small so that no plasma particles approaching within the boundaries of inter-particle distance, suffer a potential energy charge in comparison to the kT thermal energy[6]. The ion would attract electrons, increasing their density in the region, while positive ions would be repelled. The beginning of an inhomogeneous situation, one that could be induced by use of ion/particle beams, instead of lasers, to induce fusion.

The Coulomb potential is thus reduced here by virtue of the movement of charges making the plasma. When r>>d the potential becomes zero. A shielding effect ensues, as screened potential from the plasma screening effect (Fig. 1)[6].

A few special situations arise from this, but the one of interest here is, if the charge is moving with a velocity equal to or greater than the ions, but less than the electron velocity. In this case, the screening will be due to the electrons only as the ions cannot keep pace. The 'd' will be equal to $(kT_e\varepsilon_0/ne^2)^{1/2}$. This is the Debye Length, which due to above derivation, can be seen to earn the name Debye shielding distance:

$$\lambda_D = \left(kT_e\varepsilon_0/ne^2\right)^{1/2} = \sqrt[69]{T_e/n} \quad \text{S.I units} \quad (3)$$

Should the charge move faster than the electrons or ions, nothing screens it. The Debye length can be seen also the size of a sphere, so the number of charged particles within will be:

$$N_0 = \tfrac{4}{3}\pi n\gamma_D^3 = 4\pi\left(\varepsilon_0 kT_e\right)^{3/2}/e^2 n^{1/2} \quad (4)$$

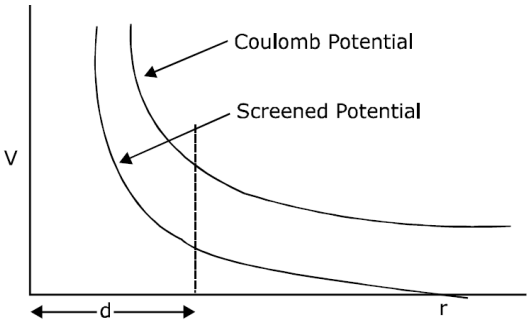

Fig. 1: Coulomb Potential between the Charges

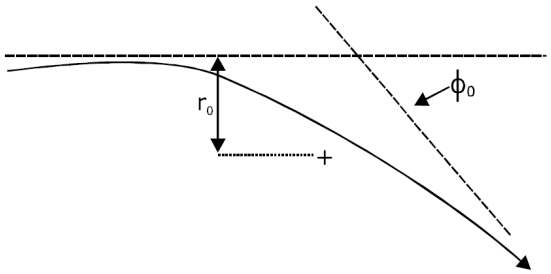

Fig. 2: Coulomb Collision of an Electron and an Ion

Charge me, at the center has potential 1/2 kT_e, the order of the thermal energy. This dimension is also relevant for the space-charge sheaths that develop where plasma come in contact with the walls of their confinement vessel.

The Debye length also relates to the plasma frequency, due to inertia causing the overshoot of the oscillating charges. The perturbation of the electrons from neutrality and subsequent oscillation, relative to the ions is situated specifically determining plasma frequency:

$$\omega_p/2\pi = \left(n_0e^2/4\pi^2\varepsilon_0 m_e\right)^{1/2} \approx \sqrt[9]{n_0} \quad (5)$$

$$\omega_p = \left(n_0e^2/\varepsilon_0 m_e\right)^{1/2} \quad (6)$$

One small, but important point, these velocities can be relativistic if $kT = mc^2$. This may occur at $T \sim 10^{10}$ K. By adding thermal effects the mechanism to allow wave packets to propagate is admitted. This is done by including the plasma pressure term[7] in the equation of motion. Thus the dispersion term, from the frequency term becomes:

$$\omega^2 = \omega_p^2 + \frac{3kT_e k_2}{m_e} \quad (7)$$

T_e, being electron temperature.

Schlüter's two fluid equations: Electrons and ions collide. Electrons are attracted to ions, with a lateral

separation of r_0 between them, the impact parameter (Fig. 2).

Time allowed for interaction: $t = \frac{r_0}{v}$ now over this time the electron's momentum will change, giving the angle $Ø_0$.

In discussing the effects of electromagnetic radiation on plasma it will be noticed, that a dichotomy exists. The energy absorbing, or reflecting, depends on whether the ions or electrons are being discussed. Clearly if fusion is the direction of the discussion, than the ions, the nuclei are going to the highlighted more. The input energy to compress the plasma will be spread over both components; hence both need to be fully treated before focusing on the actual nuclear processes. The model of envisioning plasma as the two fluids (and using Bolztmann's kinetic theory, as being used throughout here) is the work of Arnulf Schlüter[8].

In discussing the effects of electromagnetic radiation on plasma it will be noticed, that a dichotomy exists depends on whether the ions or electrons are being discussed. The model of envisioning plasma as two fluids is the work of Arnulf Schlüter. In his 1950 study, "Dynamik des Plasmas I Grundgleichungen, Plasma in gekreuzten Feldern", he explains that this dichotomy allows the plasma to be seen as an entity. "Das Plasma zieht sich dann zu einen Faden zusammem". Essentially, plasma has the ability to draw it together in one single thread (or unit).

Taking the Euler equation and setting it for electrons[5].

$$mn_e \frac{dv_e}{dt} = -n_e eE - n_e \frac{e}{c} v_e \times H - \nabla \tfrac{3}{2} n_e kT_e + mn_e v_{ei}\left(v_i - v_e\right) + K_e \quad (8a)$$

While for ions:

$$m_i n_i \frac{dv_i}{dt} = Zn_i eE + n_i \frac{Ze}{c} v_i \times H - \nabla \tfrac{3}{2} n_i kT_i - mn_e v_{ei}\left(v_i - v_e\right) + K_i \quad (8b)$$

v_i being ion velocity, v_e electron velocity, mi ion and electron mass respectively. E is the electric field, while $j_e = n_e v_e$ is the current density involved in the Lorentz force. Te and Ti terms are thermo-kinetic pressure terms, relating to the temperature of electrons and ions, as has been used before. The V_{ei}, electron-ion collision frequency, which will help, determine the viscosity as a net velocity and for the current density. Also using the neutrality (space charge), the equation of motion of plasma becomes:

$$f = m_i n_i \frac{dv}{dt} = -\nabla p + \frac{1}{c} j \times H + \frac{1}{4\pi}\left(\frac{\omega_p}{\omega}\right)^2 E \cdot \nabla E \quad (9)$$

The non-linear force, described by:

$$f_{NL} = \frac{1}{c} j \times H + \frac{1}{4\pi} \nabla . E + \frac{1}{4\pi} \nabla . \left(n^2 - 1\right) EE \quad (10)$$

is complete[5].

Genuine two fluid plasma model: When the electron cloud is pushed by the nonlinear force; the ions are subsequently dragged on by virtue of electrostatic fields. The equations:

$$v = \frac{m_i v_i + Zmv_e}{m_i + Zm}$$

$$j = e\left(n_i v_i - n_e v_e\right)$$

As a net velocity and for the current density have to be coupled with the Maxwell equations at the very least, the Poisson equation.

The first thing to emerge from research is the fact plasmas are not free from internal electric fields at the high-frequency range of an irradiating laser. This was seen in studies of cosmic and geophysical plasma's, by[9,10]. This led to a real time, collisional, non-linear generalization for these high-intensity laser fields. Transfer of energy from electrons to ions and back again, by an adiabatic compression, had to be included. Energy from the laser to electrons of ions is a vital step if a process allowing for nuclear fusion is to be realized. The process is complex, some simplification needs to be made, such as omitting minor radiation loses, these do not greatly affect fusion gain calculations. Here bremsstrahlung losses need to be included. The plasma under consideration is one-dimensional and of mainly deuterium. It includes collision produced viscosity and thermal conductivity; where Spitzer's[11] value was corrected from his value by 50 to 100 for deuterium pellets. This agreed with the electric double layer preventing electrons carrying energy off. This energy transport ceased to be electrons and was only by ion thermal conductivity. The ratio between both conductivities is:

$$\frac{m_e}{m_i} = \frac{5.4858026 \times 10^{-4}}{2.014101795} = 2.723696793 \times 10^{-4}$$

$$= \frac{0.91095310 \times 10^{-3}}{3.344548}\left(\frac{m}{10^{-27}\,kg}\right) = 2.7236965698 \times 10^{-4}$$

$$= \frac{0.5110034}{1876.139} M_e V = 2.723332569 \times 10^{-4}$$

Average value = $2.723575439\ 10^{-4}$
The square root of which is = 0.016530503

The thermal conductivity was reduced by a factor of 71 for deuterium plasma (Fig. 3). Essentially the model involves seven unknowns:

n_e electron densities	n_i ion densities
v_e electron velocity	v_i ion velocity
T_e electron temperature	T_i ion temperature

and the longitudinal electric field E, corresponding to plasma oscillations. Expressed through seven equations:

i. Continuity for electrons and ions:

$$\frac{\partial}{\partial t}\left(m_e n_e\right)+\frac{\partial}{\partial x}\left(m_e n_e v_e\right)=0 \tag{11a}$$

$$\frac{\partial}{\partial t}\left(m_i n_i\right)+\frac{\partial}{\partial x}\left(m_i n_i v_i\right)=0 \tag{11b}$$

ii. Equation of Motion[12]:

$$\frac{\partial}{\partial t}\left(n_e m_e v_e\right)=-\frac{\partial}{\partial x}\left(n_e m_e v_e^2\right)-\frac{\partial}{\partial x}\left(n_e k T_e\right)-\frac{1}{8\pi}\frac{\partial}{\partial x}\left(E_L^2+H_L^2\right) \tag{12a}$$

$$-\frac{1}{4\pi}E\frac{\partial}{\partial x}E-m_e n_e\left(v_e-v_i\right)v\lambda_D\frac{\partial}{\partial t}\left(n_i m_i v_i\right)=-\frac{\partial}{\partial x}\left(n_i m_i v_i^2\right)-\frac{\partial}{\partial x}\left(n_i k T_i\right)+\frac{Z}{4\pi}E\frac{\partial}{\partial x}E+m_i n_i\left(v_e-v_i v\right) \tag{12b}$$

Expressed as conservation of momentum[2]:

$$\frac{\partial\left(n_e m_e v_e\right)}{\partial t}=-\frac{\partial\left(n_e m_e v_e^2\right)}{\partial x}-\frac{\partial p_e}{\partial x}-n_e eE-n_e m_e v_e\left(v_e-v_i\right)+f_{NL}$$

$$\frac{\partial\left(n_i m_i v_i\right)}{\partial t}=-\frac{\partial\left(n_e m_e v_e^2\right)}{\partial x}-\frac{\partial p_i}{\partial x}-n_i ZeE+n_e m_e v\left(v_e-v_i\right)+\frac{m_e}{m_i}f_{NL}$$

iii. Conservation of Energy:

$$\frac{\partial}{\partial x}\left(n_e\tfrac{3}{2}kT_e\right)=-\frac{\partial}{\partial x}\left(n_e v_e\tfrac{3}{2}kT_e\right)-\tfrac{3}{2}\frac{k}{m_e}T_e n_e\frac{\partial}{\partial x}v_e+\frac{1}{m_e}\frac{\partial}{\partial x}\left(K_e\frac{\partial T_e}{\partial x}\right)-\tfrac{3}{2}\frac{k}{m_e}n_e\frac{T_e-T_i}{\tau}\frac{1}{m_e}W \tag{13a}$$

$$\frac{\partial}{\partial t}\left(n_i\tfrac{3}{2}kT_i\right)=-\frac{\partial}{\partial x}\left(n_i v_i\tfrac{3}{2}kT_i\right)-\tfrac{3}{2}\frac{k}{m_i}T_i n_i\frac{\partial}{\partial x}v_i+\frac{1}{m_i}\frac{\partial}{\partial x}\left(K_i\frac{\partial T_i}{\partial x}\right)-\tfrac{3}{2}\frac{k}{m_i}n_e\frac{T_e-T_i}{\tau} \tag{13b}$$

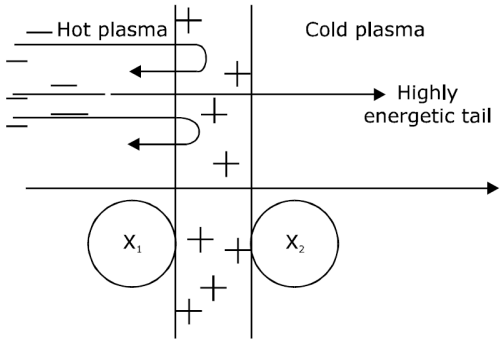

Fig. 3: Genuine two fluid plasma model

iv. $$\frac{\partial E}{\partial x}=-4\pi e\left(n_e-Zn_i\right) \tag{14}$$

Initial conditions and boundary conditions need to be put, which are time dependant with regards to the laser, i.e. Pulsed. This has to be evaluated for each time step by the spatial dependence of W, the power density for energy transfer, as a solution of Maxwell's equations. We can be viewed from the fluid mechanic point of view to be like the external heat deposited per unit volume; assuming no external forces[13] viz:

$$\frac{\partial}{\partial t}\left[p\left(\varepsilon+\tfrac{1}{2}v^2\right)\right]+\mathrm{div}\left[pv\left(h+\tfrac{1}{2}v^2\right)\right]+\mathrm{div}q=W$$

It includes all reflections and absorption properties belonging to the inhomogeneous plasma. All the equations and material to this point have been used to develop computer codes, of varying accuracy. Data gleaned from varying experiments, also adds to fill or test the accuracy of these codes. As the cost of such experiments is prohibitive. While the power of the computers involved limits access by many. To fully describe plasma's behavior, like that of the fluid, the thermodynamic state and velocity of flow are required[13, 14]. The state variables, usually two such as pressure, density; plus three vector components of velocity are usually all that is required for the equation of state. The variables being independent of each other. They form the dependant variables against the independent variables of space and time.

Any plasma formed in the code or reality expands, thus in one dimension there is as many negative values as positive values of velocity on the average. The magnitudes are usually of the same order. Taking a 1 keV deuterium plasma, starting at time zero and developing at a density of near critical ($10^{21}cm^3$) with a temperature of order 10^{70}K for both ions and electrons. The laser intensity is taken to be that of a neo-dymium glass laser of 10^{16} Wcm^{-1} (square pulse) with wavelength, 1.06 μm. The density being important, as it changes the refractive index and can result in total reflection of the source of the driving force[15].

To bring about fusion it is required that the nuclei of the deuterium are forced together so as to overcome the Coulomb force of repulsion. To bring them into proximity of a Fermi (10^{-15} meter). This means increasing the density of the ions, as it is the ions, which constitute the site of the nuclei. Examining some of the variables it can be seen the longitudinal electric field is zero at the outset, Fig. 4. The electron fluid expands faster, thus developing an electric field. The electrons change direction, as discussed earlier, leading to an oscillation, which appears as the plasma frequency. This being electron density dependant. Given enough time the field becomes a uniform internal one of 10^6 Vcm^{-1} [12,14]. Spatially this occurs over 10^{-3}cm.

Once the laser is turned on at 0.6 p sec, longitudinal Langmuir oscillation results. Their amplitude is about one-tenth the transverse laser field amplitude. Unfortunately non-conservative characteristics result when very strong oscillations occur due to the laser. This has been explored by workers such as[16,14,17]. Indeed Umstadter found using a 25TW-pulsed laser produced 30 MeV electrons in vast numbers and the plasma acceleration mechanism resulted[14]. Took the conservation equations and derived the following from the oscillation equation:

$$\frac{\partial^2 E}{\partial t^2} + v\frac{\partial E}{\partial t} + \omega^2_{p0}E = E_{s0}\omega^2_{p0} + \frac{4\pi e}{Me}\frac{\partial}{\partial x}\frac{E_L^2 + H_L^2}{8\pi} + 4\pi ev\left(n_i v_i - Zn_e v_e\right) \quad (15)$$

Where:

$$E_{s0} = \frac{4\pi e}{\omega^2_{p0}}\left[\frac{\partial}{\partial x}\left(\frac{3n_i kT_i}{m_i} + Zn_i v_i^{\,2}\right) - \frac{\partial}{\partial x}\left(\frac{3n_e kT_e}{m_e} + n_e v_e^{\,2}\right)\right]$$

$$\omega^2_{p0} = 4\pi e^2\left(\frac{n_e}{m_e} + \frac{z^2 n_i}{m_i}\right)$$

The solution of which are the longitudinal electric fields, the electrostatic of Langmuir, termed E_S:

$$E_s = \frac{4\pi e}{W|_p^2}\left[\frac{\partial}{\partial x}\left(\frac{3n_i kT_i}{m_i} + Zn_i v_i^{\,2}\right) - \frac{\partial}{\partial x}\left(\frac{3n_e kT_e}{m_c} + n_e v_e^{\,2}\right) + \frac{1}{m_e}\frac{\partial}{\partial x}\frac{E_L^2 + H_L^2}{8\pi}\right]\left(1 - \exp\left(-vt/2\cos\omega_e t\right)\right) + \frac{\omega_p^2 - 4\omega^2}{\left(\omega_p^2 - 4\omega^2\right)^2}\frac{4\pi e}{m_e}\frac{\partial}{\partial x}\left|\left(E_L^2 + H_L^2\right)\cos 2\omega t\right. + \frac{2v\omega}{\left(\omega_p^2 - 4\omega_2\right)^2}\frac{4\pi e}{m_e}\frac{\partial}{\partial x}\left|\left(E_L^2 + H_L^2\right)\sin 2\omega t\right. \quad (16)$$

Other forms of which appear in[18]. The original idea from workers like[19]. This would suggest one should see rippling through the small plasma sample (25 μm), over very brief time periods (0.5 to 1.5 p sec) once energy is being inputted from a laser. This rippling should be evident from the bunching and dragging of the plasma. The density profile should reflect it and hence phase reflection would be expected at these ripples, this in turn halting the acceleration, thus the hydrodynamic disappearing of the ripple within picoseconds[12,20,21].

Figure 4 shows the zero internal fields. At 1.1 picoseconds the field builds rapidly (over 0.2 picoseconds) and at the virtual surface of the tiny piece of plasma that is within the first 8 micrometres. The first field peaks at approximately 10^8 Vcm^{-1}, the field dropping off from 20 micrometres. The movement of the electrons surrounding those "trailing behind" ions builds the field over this distance. In reality a very short distance, nearly half an interatomic distance. Clearly the graph shows a polarity reversal at 7.5 micrometres and over time 1.2 to 1.5 picoseconds. This is evidence for the direction undertaken by the electrons and hence the ions. This is a ripple effect as can be seen by the diminished, but still visible, ripple from 10 to 20 micrometres. By 25 micrometres there appears to be little field, but a more sensitive probe should detect an ever-decreasing undulation of the field, given a larger piece of plasma.

The actual electromagnetic energy density of the laser field is shown in Fig. 5. $\left(E_s^2/8\pi\right)$. This graph gives an indication of how much energy is actually deposited by the laser and where/when is it available. Pulsation is again detected both over time and through distance. It can be seen to be time dependant starting at 0.6 p sec, dropping off and reforming in 0.7 and so on. The maxima would correspond to strong penetration. Each ripple corresponds to acceleration stopping (Fig. 6a and b). This is the stuttering effect reported by Maddever and also Hora. It shows the energy is not being evenly delivered over time and throughout the plasma. The peak is reached at around 0.9 picoseconds, dropping rapidly down by 1.1 picoseconds, then a smaller rise at 1.5 picoseconds. This same pulsation in or stuttering is evident through distance. The greatest density or deposits of energy being near the surface at 4-5 micrometres. Looking over time, the maximum densities occur at this distance. Further suggesting the energy does not penetrate very deeply and making pellet size a critical factor in obtaining fusion. The rippling shows the density changes, which result in reflection of the laser pulses. From the laser point of view a smoother delivery of energy is required. The field structures so far noted are the results of the nonlinear force. This same force will be the determining force for all the ions (and electron) movement determining the graph shape and are results derived from the 'genome' two-fluid model.

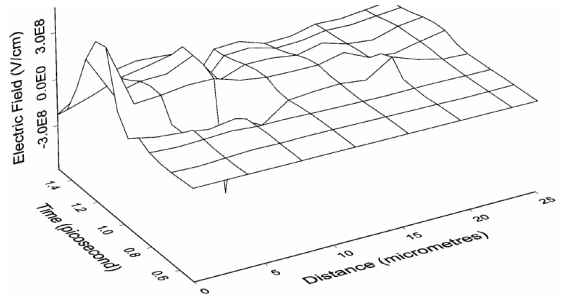

Fig. 4: Electric Field inside the Plasma Changing Over Time. The Field Being Generated around the Focus of the Laser Beam in the Plasma

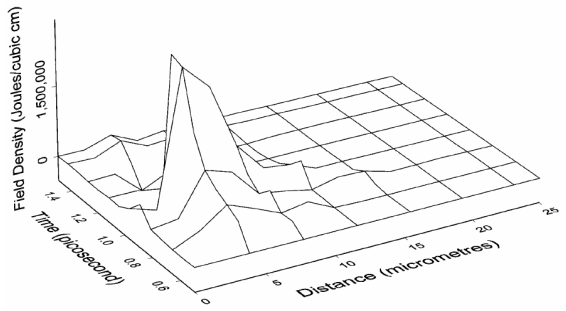

Fig. 5: Electric Field Density of the Laser. The Energy Concentration is in Joules per Cubic Centimeter. A Caviton can be seen at about 0.4 Picosecond and at a Distance of 3.5 Micrometre

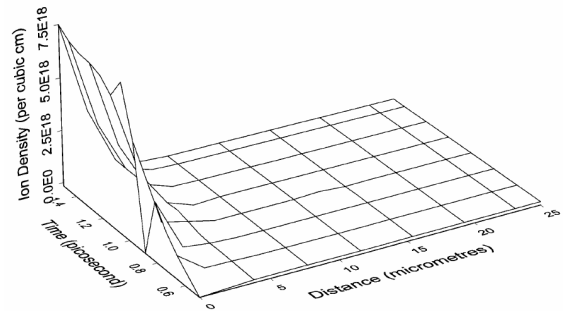

Fig. 6a: Ion Density, per Cubic Centimeter. The Number of Ions being taken in the Order in 10^{18}

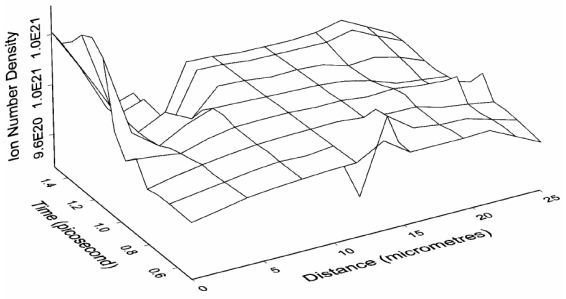

Fig. 6b: Ion Number Density Shows the Ripple Effect Better Than Ion Density

The field density pulsation should also be seen in the ion density changing, thus effecting reflectivity. Low ion density should relate to higher laser field energy densities. By comparing Fig. 5 and Fig. 6a it can be seen the field values so micrometres. The wall of ions built up on the plasma surface accumulated over a few picoseconds. The movement to that position was against the direction of the laser beam. As noted a slight ripple is seen at a distance of 4-5 micrometres. Little effect is seen then until 12.5 or so micrometres on an almost unperceivable 'bump'. One would speculate that given more time and continuing irradiation this iron wall would migrate through the plasma. The pulse is better defined in Fig. 6b.

It was suggested by Weibel in the early 1950's, that this wall could be made to surf on the field wave. The ideas being to have an input wave collision with a reflective wave and hence fuse the ions. Certainly, on first examination of this idea, it would seem feasible that if enough energy could be imparted to the two opposing waves that Coulomb force of repulsion could be overcome, the ions brought within a Fermi and then the nuclear force would take over fusing the nuclei. The time over which this event took would be crucial and it is here the idea fails, (Hora, oral communication). One still feels the basic idea could be explored further.

Figure 7 shows the vector nature of ion velocity. There is little movement until 0.6 picoseconds. Until that time, when the laser is activated the ions are uniformly travelling in all directions at relatively slow velocities. Taking one dimension they are travelling at –19000 cms^{-1} and 19000 cms^{-1}, uniform expansion of the 25-micrometre plasma. As the laser energy sets up the non-linear force the ions are greatly accumulated diminishing the original expansion velocities, even those quoted which occur on the periphery. For example, after 1.0 picoseconds and 2.5 micrometres the speed (magnitude of velocity) reaches 9.0×10^{6} cms^{-1}, i.e. around 9000 ms^{-1}, 32,400 kilometers an hour or nearly three times the speed of sound in air. This expressed it in terms that the average person could appreciate; like "jet plane" speeds. At 1.1 picoseconds this has increased to 9.5×10^{6} cms^{-1} or 95 kms^{-1} (342,000 kmh^{-1}).

Clearly Fig. 7 shows the oscillating nature if the values. From the surface rise over time to a high positive value, 4.25 x 10^{6} cms^{-1}, the graph plummets, to high negative values $-8x10^{6}$ cms^{-1}. This shows the ions have charged in one initial direction only to do an about face and charge on the other, through a distance of about 10 micrometres. In the next 5 or so micrometres the direction is again reversed, but by 15-20 micrometres the forces seem to suffer a delay in their effect on the ions. Only by about 17.5 micrometres is the next undulation building and then not as dramatic. It can be seen that it takes time to build the moving walls of ions. In addition the largest proportion of effect is in the area of immediate contact with the laser. It is further noted that the response time to cause a change in direction is very quick, a few picoseconds. Further the space required for

the turnaround is short, nearly half a Fermi (less by an order of magnitude). A point of curiosity is the distance created between packets of undulation, some 5 micrometres. Given the Debye length is[22]:

$$\lambda_D = \left(\pi n e^2\right)^{1/2}$$
$$= 7.43\times10^2 T^{1/2} n^{-1/2}\text{cm, sub in } 10^{07}\text{ K}$$
$$= 7.43\times10^2 \left(316.27766\right) N^{-1/2}\text{cm}$$
$$= 2349572.301 n^{-12}\text{cm}$$

Taking in to be an Avogadro number of ions:

$$= \frac{2349572.301}{7.76.219069\times10^{11}}$$
$$= 3.022713883\times10^{-6}\text{cm}$$
$$\approx 3\times10^{-8}\text{m or 0.03 micronetres}$$

In a hot plasma $\left(T_e V \approx 10^2, n = 10^{14}\right), \lambda_D = 7\times10^{-4}\text{cm}$ for thermonuclear $\left(T_e V \approx 10^4, n = 10^{15}\right), \lambda_D = 2\times10^{-3}\text{cm}$ [22]. For the sample chosen, at temperature chosen, n = 10^{21}cm^{-3}, λ_D becomes ≈ 0.743 micrometres. Given the theoretical value of thermal ion velocity is:

$$v_{Ti} = (kT_i / m_i^{1/2} = 9.79\times10^5 \mu^{11_2} T_i^{11_2}\text{cms}^{-1}$$

Where $\mu = m_i / m_p$ which form ${}_1^1H$ is 1.0080602 approximately, while ${}_1^2H$ being 2.016992018.

Thus the velocity is for:

$${}_1^1H : 3.071\times10^9\text{cms}^1 \quad {}_1^2H : 1.5\times10^9\text{ cms}^{-1}$$

These values are in reasonable agreement with those of maximum value in Fig. 7.

The discrepancy probably lies in the units used. During the time that these graphs represent the temperature remains reasonably constant. This is in accord with the concept of adiabatic expansion. It is taken as 1×10^7 K at the start, over the next time unit, the 0.6 picoseconds it barely changes.

Figure 8 shows a rise of 0.7 to 0.9 picoseconds on the surface. It is over the 0.7 to 1.0 picoseconds the temperature rise for the electrons to migrate through the plasma. This creates a hot spot, a depth of 7.5 to 10 micrometres. This translates to maximum thermal movement of the electrons and corresponds the 'calm period' of ion velocity in Fig. 8. This could be interpreted to illustrate a time delay in electron movement setting up a field to drag the ions. Certainly electron temperature is at base level when ion velocity is undergoing its greatest changes.

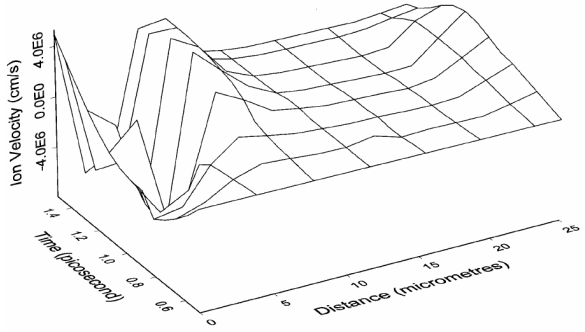

Fig. 7: Ion Velocity in Centimeters, Illustrating the Surface Effect of the Initial Activity with "Calm Period" Leading to Next Rippling Effect

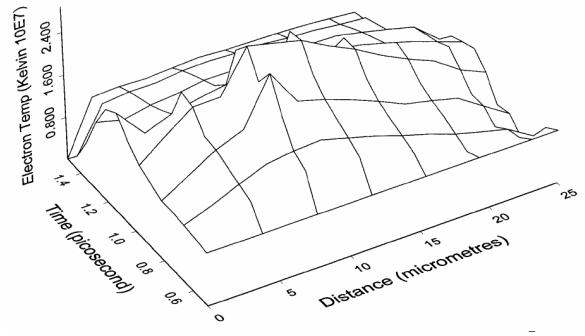

Fig. 8: Electron Temperature in Units of 10^7 Degrees Kelvin

The electrons being at least 2,000 times lighter than ions are more easily affected. Writers such as Hora and Lalousis, claim the effect on the ion is of the order of m_i/m_e less. The equi-partition time given by Spitzer[14] is around 3×10^{-10} seconds for the parameters used.

The variables were chosen from the two fluid models, as expressed in the continuity equations (11a and 11b); and the equations of motion[2]. Due to the very limited computing power available, numerically discrete variables were chosen based on earlier computerized models using the step Lax-Wendroff method,[14]. In these the stepwise grid point formula, coupled with boundary conditions, could be used to find values for fNL. The electric field, changing over time, derives from the Poisson's equation:

$$\frac{\partial E}{\partial t} = 4\pi e\left(n_e v_e - Z n_i v_i\right)$$

These values were simulated using the SPLUS package and each set against discrete time units. This was done to better highlight the rippling in the plasma as discussed by many previous authors (Hora and Lalousis). Many of these values agreed with these previous workers, but the idea here was to view all of them over time, howbeit, very short units of it.

CONCLUSION

This study has investigated the nature and properties of plasma by a mathematical approach. It focused in on the movement of electrons and ions in fully ionized plasma. Electrostatic forces were added to the list of forces involved. The non-neutrality of inhomogeneous plasma was examined. The distances between the particles and the effect of collisions between were viewed in terms of electric currents being evident in any plasma. Models, such as Schlüters two fluid models were examined along with the non-linear force. From Schlüters two fluid models emerged the "genuine" two fluid plasma models. The study used the two fluid models to examine internal electric fields, the plasma frequency and its relation to a laser frequency. The simulations in the study analyzed the key variables of ion density, velocity, electric field densities and temperature over time. These variables were also looked at with regards to the depth of penetration of the laser beam. This was viewed against the background of the oscillations set up in plasmas by the ions pursuing the moving electrons.

REFERENCES

1. Hora, H., H. Azechi, S. Eliezer, Y. Kitagawa, J.M. Martinez-Val, K. Mima, M. Murakami, K. Nishihara, M. Piera, H. Takabe, M. Yamanaka and T. Yamanaka, 1998. Fast Ignitor with Long Range DT Ion Energy Deposition Leading to Volume Ignition. Laser Interaction and Related Plasma Phenomena, 13th Int. Conf. Ed Campbell, E.M., Miley, G.H.
2. Hora, H., 1991. Plasma's at High Temperature and Density. Springer-Verlag.
3. Ginzburg, V., 1970. The Propagation of Electromagnetic Waves in Plasma's. 2nd Edition. Pergamon Press.
4. Maecker, H., 1963. Theory of Thermal Plasma and Application to Observed Phenomena. An Introduction to Discharge and Plasma Physics, U.N.E, Armidale.
5. Hora, H. and M. Aydin, 1992. Physical Review A, 45, 6123.
6. Somerville, J., 1964. Some Fundamental Properties of Plasma's. An Introduction to Discharge and Plasma Physics, U.N.E, Armidale.
7. Brennan, M. H., 1964. Some Fundamental Properties of Plasmas. Introduction to Discharge Plasma Physics, UNE, Armidale.
8. Schlüter Arnulf, 1949. Dynamik des Plasma's I. Zeitschr. Naturforsch A5, 72.
9. Alfven, H., 1981. Cosmic Plasmas. Van Reidel, Dordrecht.
10. Falthammer, C.G., 1988. Laser and Particle Beams. 6, 437.
11. Spitzer, L., 1962. Physics of Fully Ionized Gases. 2nd Edition, Wiley.
12. Hora, H., 2000. Laser Plasma Physics Forces and the Nonlinearly Principle. SPIE Press.
13. Cairns, R.A. And J. J. Sanderson, 1980. Fluid Codes from Laser-Plasma Interactions. Proceeding the 20th Scottish University Summer School in Physics 1974, SUSSP Pub.
14. Lalousis, P. And H. Hora, 1983. First Direct Electron and Ion Fluid Computation of High Electrostatic Fields in Dense Homogenous Plasma's with Subsequent Non-linear Laser Interaction. Laser and Particle Beams 1: 28-304.
15. Maddever, R., B. Luther-Davies and R. Dragila, 1990. Phys. Review Letters, 80, 261.
16. Umstadter, D., 1996. Terawatt Lasers Produce Faster Electron Acceleration. Laser Focus World Feb 1996.
17. Eliezer, S. And H. Hora, 1989. Double Layer in Laser Produced Plasmas. Physics Reports, 172, 339-407. North Holland Amsterdam.
18. Goldsworthy, M.P, H. Hora and R.J. Stening, 1990. Double Layer Effects Causing Nearly Uniform Striated Second Harmonic Emission from a Laser Irradiated Plasma Corona. Laser and Particle Beams, 8: 33-49.
19. Weibel, E.S., 1958. A Note on the Confinement of a Plasma by R.F. Fields. J. Electr. Contr. 5, 435.
20. Hora, H., 1977. Physics of Laser Driven Plasmas, Wiley-Interscience Publication.
21. Eliezer, S., H. Hora, F. Green, P. Lalousis and H. Szichman, 1988. Acceleration of Electrons by Double Layers in Laser- Plasma Interaction. Vol 7, Laser Interaction and Related Plasma Phenomena.
22. Huba, J.D., 2000. NRL Plasma Formulary. Naval Research Laboratory, Washington DC 20375-5320.